

Turn-on Phosphorescence by Metal Coordination to a Multivalent Terpyridine Ligand: A New Paradigm for Luminescent Sensors

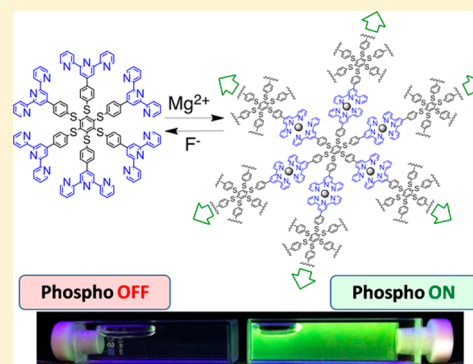
Andrea Fermi,^{†,‡} Giacomo Bergamini,[†] Myriam Roy,[‡] Marc Gingras,^{*,‡} and Paola Ceroni^{*,†}

[†]Department of Chemistry "G. Ciamician", University of Bologna, 40126 Bologna, Italy

[‡]Aix-Marseille Université, CNRS, CINaM UMR 7325, 163 Ave. de Luminy, 13288 Marseille, France

S Supporting Information

ABSTRACT: A hexathiobenzene molecule carrying six terpyridine (tpy) units at the periphery has been designed to couple the aggregation induced phosphorescence, displayed by the core in the solid state, to the metal binding properties of the tpy units. Upon Mg^{2+} complexation in THF solution, phosphorescence of the hexathiobenzene core is turned on. Metal ion coordination yields the formation of a supramolecular polymer which hinders intramolecular rotations and motions of the core chromophore, thus favoring radiative deactivation of the luminescent excited state. Upon excitation of the $[Mg(tpy)_2]^{2+}$ units of the polymeric structure, sensitization of the core phosphorescence takes place with >90% efficiency. The light-harvesting polymeric antenna can be disassembled upon fluoride ion addition, thereby switching off luminescence and offering a new tool for fluoride ion sensing. This unique system can, thus, serve as cation or anion sensor.



INTRODUCTION

2,2':6',2''-Terpyridine (tpy) is one of the most investigated ligand for d-block metal ions because it yields highly stable complexes with interesting optical, electronic, and magnetic properties.^{1,2} Because of its three coordinating N atoms and the ease of substitution at the 4'-position, it is ideal for the construction of linear, rigid arrays with univocally determined structure with d^6 -metal ions.³ Thus, it has been widely employed in dyads and linear polynuclear metal complexes,⁴ grids and racks,⁵ and metallomacrocycles,⁶ as well as metal coordination polymers.^{2a,7,8} Terpyridine is weakly luminescent ($\Phi_{em} = 3 \times 10^{-3}$)⁹ and a variety of chromophores have been appended to it to combine luminescence and metal binding properties.^{1,2} In the past few years, a novel class of luminophores displaying aggregation induced emission (AIE)¹⁰ has attracted increasing attention. In most cases, the emission enhancement is due to an aggregation or a crystallization, which causes restriction of intramolecular motions.¹¹ These chromophores, thus, offer new potentialities for solid-state optical devices, such as organic light-emitting diodes (OLEDs) for sensors and luminescent probes in materials or in biological sciences.¹⁰

Following those lines, the combination of AIE chromophores and metal ion ligands has recently been explored.¹² However, to the best of our knowledge, no example is described in which the metal ion coordination switches on phosphorescence of an organic chromophore which is not directly involved in metal ion coordination. Phosphorescent AIE systems are particularly interesting: for sensing, they allow time-gated detection, which eliminates autofluorescence of the sample; for OLEDs

phosphorescent materials enable a theoretical maximum efficiency of 100% compared to 25% for fluorescent materials.

In the present paper, we report an example of a molecule (**1**, Scheme 1) consisting of a benzene core carrying six phenyl-terpyridine units connected by a sulfur atom. This multivalent ligand has been designed to combine the metal coordination ability of the tpy units to the aggregation induced phosphorescence properties of the previously investigated molecule **2** (Scheme 1).¹³ The latter is not emissive in solution, but it is among the most phosphorescent organic solids ($\Phi_{em} = 1$),¹⁴ due to restricted intramolecular rotations and conformational mobility in rigid environment. Coordination of Mg^{2+} ions by **1** leads to the appearance of a similar phosphorescence band also in air-equilibrated fluid solution due to the formation of a metal-coordination polymer, in which intramolecular rotation is restricted. Moreover, the polymeric structure performs as a light-harvesting antenna: excitation of the $[Mg(tpy)_2]^{2+}$ units sensitize the hexathiobenzene core luminescence with almost unitary efficiency. The luminescence can be switched off again by disassembling the supramolecular structure upon fluoride addition, which sequesters Mg^{2+} ions.

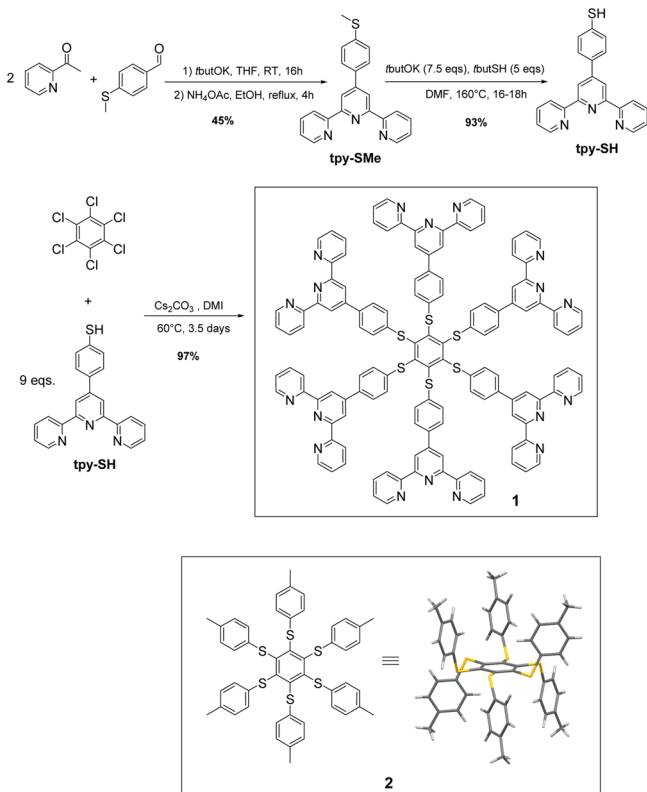
EXPERIMENTAL SECTION

Materials and General Procedures. All reagents, solvents and chemicals were purchased from Sigma-Aldrich, Fisher, or Alfa-Aesar and used directly unless otherwise stated (purity: reagent or analytical grade). Solvents were stored for several days over freshly activated 3 Å molecular sieves (activated for 3 h at 250 °C). Triethylamine and

Received: February 13, 2014

Published: April 11, 2014

Scheme 1



other amines were freshly distilled over KOH prior to use or distilled and stored over KOH under argon. HPLC analysis were performed with a Jasco HPLC system (Jasco France, Nantes) fitted with a PU 980 intelligent pump equipped with a LG 980–02 tertiary gradient unit, a DG 980–50 line degasser, a 7725i Rheodyne injection valve with a 20 μL loop, a UV 975 intelligent UV–vis detector. Infrared absorption spectra were directly recorded on solids or neat liquids on a PerkinElmer Spectrum 100 FT-IR Spectrometer equipped with a universal ATR accessory (contact crystal: diamond). Uncorrected melting points were recorded on a IA9200 digital melting point apparatus from Thermofischer Scientific (Electrothermal) after a calibration certification with standards. ^1H NMR (250.13 MHz) and ^{13}C NMR (62.90 MHz) spectra were recorded on a Bruker Avance 250 spectrometer at 300 K in the mentioned deuterated solvents. ^1H NMR signals of the residual protic solvent CHCl_3 at 7.26 ppm and CH_2Cl_2 at 5.32 ppm were used as internal references, along with TMS. As for ^{13}C NMR spectra, the central resonance of the triplet for CDCl_3 at 77.36 ppm and the central resonance of the quintuplet for CD_2Cl_2 at 54.0 ppm were used as internal references. High resolution mass spectra were recorded at the Spectropôle de Marseille (France) in triplicate with double internal standards. Oligomers of poly(propylene glycol) were used as internal standards. Ionization was facilitated by some adducts with Ag^+ , NH_4^+ , or Na^+ ions. Two spectrometers were used: SYNAPT G2 HDMS (Waters) instrument equipped with an ESI source and a TOF analyzer in a positive mode and a QStar Elite (Applied Biosystems SCIEX) instrument equipped with an atmospheric ionization source (API).

Synthesis. For details on the synthetic procedures for **tpy-SH** and **tpy-SMe**, see Supporting Information.

1,2,3,4,5,6-Hexakis(4-([2,2':6',2''-terpyridin]-4'-yl)phenylthio)benzene (1). In an oven-dried round-bottom flask were placed hexachlorobenzene (41.3 mg, 0.145 mmol, 1.00 equiv), 4'-[4-(mercapto)phenyl]-2,2';6',2''-terpyridine (**tpy-SH**) (436.9 mg, 1.280 mmol, 8.83 equiv), and dry Cs_2CO_3 (588.2 mg, 1.805 mmol, 12.4 equiv). All reagents were freshly dried under high vacuum for about 30 min prior to use them. Under an argon atmosphere, dry 1,3-dimethyl-2-imidazolidinone (DMI, 5.0 mL) was then injected in one portion at

20 °C and the mixture was vigorously stirred at 60 °C (oil bath temperature) for 4.5 days. After cooling down at 20 °C, the suspension was poured into a 1 M NaOH aqueous solution (20 mL). A bright yellow solid precipitated, which was separated by filtration, washed several times with H_2O , and dried under high vacuum. It was then titrated while vigorously stirring in ethanol to afford a pure solid (298.3 mg, 0.141 mmol, 97% yield).

MP: 394–397 °C (bright yellow powder); **FT-IR** (ATR diamond contact; solid sample): 3050 (CH), 3012 (CH), 1583 (tpy), 1564 (tpy), 1467 (CH), 1384 (CH) cm^{-1} . **^1H NMR** (250 MHz, CDCl_3 , ppm): δ = 7.11 [ddd, 12H, 4J (H,H) = 1.2, 3J (H,H) = 4.8, 3J (H,H) = 7.4 Hz], 7.19 [dapp, 12H, 3J (H,H) = 8.4 Hz], 7.68 [ddd, 12H, 4J (H,H) = 1.8, 3J (H,H) = 7.8, 3J (H,H) = 7.8 Hz], 7.74 [dapp, 12H, 3J (H,H) = 8.4 Hz], 8.36 [d, 12H, 3J (H,H) = 7.9 Hz], 8.46 [bd, 12H, 3J (H,H) = 5.7 Hz], 8.48 [s, 12H]. **^{13}C NMR** (62.90 MHz, CDCl_3 , ppm): δ = 118.6, 121.3, 123.7, 128.4, 129.2, 136.7, 137.0, 138.6, 148.5, 149.1, 149.3, 155.7, 156.2. **MS:** MALDI-ToF MS (DCTB matrix in DCM, laser l = 337 nm, + mode) for $\text{C}_{132}\text{H}_{84}\text{N}_{18}\text{S}_6$ calcd. 2113.5 Da, found m/z 2113.5 $[M]^+$. MALDI-ToF (DCTB matrix in DCM, NaI, laser l = 337 nm, + mode) for $\text{C}_{132}\text{H}_{84}\text{N}_{18}\text{S}_6 + \text{Na}^+$ calcd. 2136.6 Da, found m/z 2136.6 $[M+\text{Na}]^+$.

Photophysical Measurements. The experiments were carried out in air-equilibrated tetrahydrofuran solution at 298 K unless otherwise noted. Luminescence measurements at 77 K were performed in dichloromethane/methanol (1:1 v/v). UV–vis absorption spectra were recorded with a PerkinElmer 140 spectrophotometer using quartz cells with path length of 1.0 cm. Luminescence spectra were performed with a PerkinElmer LS-50 or an Edinburgh FLS920 spectrofluorimeter equipped with a Hamamatsu R928 phototube. Lifetimes shorter than 10 μs were measured by the above-mentioned Edinburgh FLS920 spectrofluorimeter equipped with a TCC900 card for data acquisition in time-correlated single-photon counting experiments (0.5 ns time resolution) with a D_2 lamp. Longer lifetimes were measured by the PerkinElmer LS-50. Emission quantum yields were measured following the method of Demas and Crosby¹⁵ (standard used: $[\text{Ru}(\text{bpy})_3]^{2+}$ in aqueous solution).¹⁶ For solid samples, emission quantum yield was calculated from corrected emission spectra registered by an Edinburgh FLS920 spectrofluorimeter equipped with a barium sulfate coated integrating sphere (4 in.), a 450W Xe lamp (λ excitation tunable by a monochromator supplied with the instrument) as light source, and a R928 photomultiplier tube, following the procedure described by De Mello et al.¹⁷ The estimated experimental errors are 2 nm on the band maximum, 5% on the molar absorption coefficient and luminescence lifetime, 10% on the emission quantum yield in solution, and 20% on the emission quantum yield in solid.

Morphological Characterization. The determination of the hydrodynamic diameter distributions of the nanocrystals was carried out from DLS measurements with a Malvern Nano ZS instrument with a 633 nm laser diode. Samples were housed in a quartz cuvette of 1 cm optical path length using THF as solvent. The width of DLS hydrodynamic diameter distribution is indicated by PDI (polydispersion index). AFM imaging was performed using a Nanoscope Multimode 8 (Bruker, Santa Barbara, U. S. A.) equipped with a 15 μm piezoelectric scanner. The AFM was operated in tapping mode and in peak-force tapping mode.

RESULTS AND DISCUSSION

Molecule **1** was obtained after a persulfuration of hexachlorobenzene in a 97% yield by means of six consecutive substitutions of chlorine atoms (99.5% yield per reaction) by the anions of **tpy-SH** (Scheme 1).¹⁸ The latter thiol was prepared from **tpy-SMe** after an effective transthioetherification (93% yield) from a nucleophilic demethylation with tertiothiolate anions.¹⁹ **Tpy-SMe** was itself synthesized according to the literature in a one-pot process (45% yield) from 2-acetylpyridine and 4-(methylthio)benzaldehyde.²⁰ Finally, compound **2** was synthesized according to the literature.²¹

The absorption spectrum of **1** in THF solution shows a band with maximum at ca. 280 nm typical of the tpy chromophore, as evidenced from the comparison with the spectrum of tpy-SMe, and a tail extending up to 450 nm, present also in the model compound **2** (Figure 1).

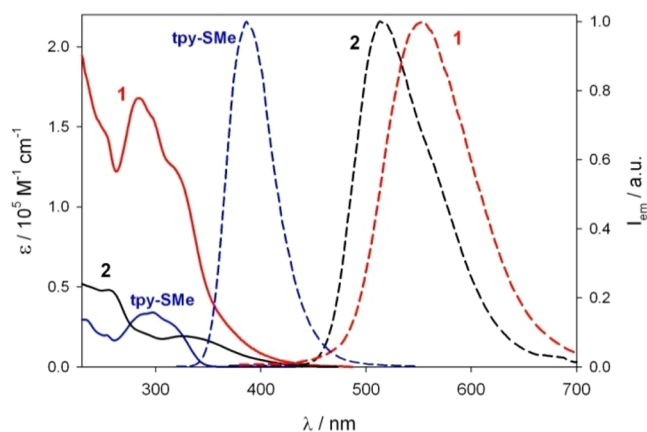


Figure 1. Absorption spectra (solid lines) in THF solution of **1** (red line), **2** (black line), and tpy-SMe (blue line). Dashed lines represent the normalized phosphorescence spectra of **1** and **2** in the solid state, as a powder, and the fluorescence spectrum of tpy-SMe in THF solution. $\lambda_{\text{ex}} = 330$ nm.

Compound **1** and **2** are practically nonluminescent in fluid solution ($\Phi_{\text{em}} < 10^{-3}$) and exhibit an intense emission in the solid state as a powder. This radiative deactivation is a phosphorescence in agreement with the relatively long lifetimes of the corresponding emitting excited states ($\tau_1 = 1.7$ and $\tau_2 = 11.6$ μs for **1** and $\tau = 3.0$ μs for **2**¹³). The switch on of luminescence going from solution to solid state can be attributed to restriction of intramolecular rotations and motions, as previously discussed for **2**. It can be attained also in an extremely diluted rigid matrix at 77 K: compound **1** shows a band with maximum at 500 nm and a lifetime of 3.5 ms in $\text{CH}_2\text{Cl}_2/\text{CH}_3\text{OH}$ 1:1 (v/v) matrix. In the case of **1**, the emission band recorded in the solid state is red-shifted and exhibits a much lower emission quantum yield (0.02, Table 1) compared with that of **2**. This suggests that, in the case of **1**, intramolecular rotation is not completely hindered in the solid state likely because the tpy units appended at the periphery yield a less compact structure compared to that of **2**.

Upon titration of a 3.3×10^{-6} M air-equilibrated THF solution of **1** with $\text{Mg}(\text{ClO}_4)_2$, profound changes of the absorption and emission spectra are observed (Figure 2). A red-shifted absorption band at ca. 380 nm increases with an isosbestic point at 326 nm. Upon excitation at this wavelength,

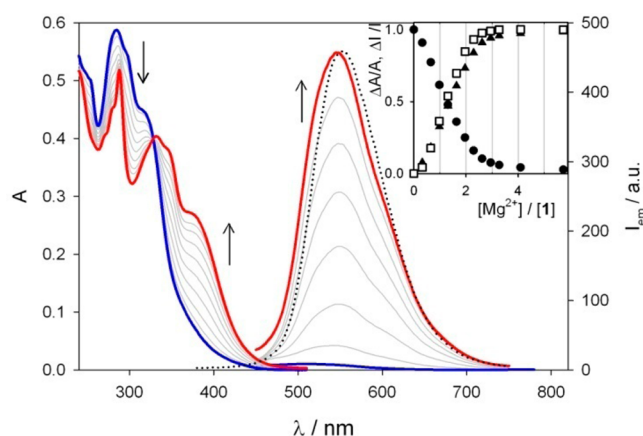


Figure 2. Absorption (left) and phosphorescence spectra (right) of a 3.3×10^{-6} M solution of **1** in air-equilibrated THF solution upon titration with a 2.70 mM acetonitrile solution of $\text{Mg}(\text{ClO}_4)_2$: blue line (0 equiv), red line (3.2 equiv). Inset shows the normalized absorption changes at 299 (solid circles) and 375 nm (solid triangles) and emission intensity changes at 545 nm (empty squares). $\lambda_{\text{ex}} = 326$ nm (isosbestic point). Dotted line represents the emission spectrum of **1** as a powder.

a new phosphorescence band at 545 nm appears. Both absorption and emission intensities (Figure 2 inset) reach a plateau at ca. 3 equiv of Mg^{2+} ions per **1**. The final emission spectrum (red line, Figure 2) corresponds to an emission quantum yield of 0.10 and it is superimposed to that of **1** as a powder (dotted line, Figure 2). Moreover, the corresponding lifetimes are 1.7 and 5.3 μs in air-equilibrated solution, very similar to that of **1** as a powder (Table 1). These results point out that the emission is a phosphorescence typical of the hexathiobenzene core of molecule **1**.

Similar absorption changes are observed for tpy-SMe upon titration with $\text{Mg}(\text{ClO}_4)_2$ (Supporting Information Figure S9), but in this case, no phosphorescence is observed. The fluorescence of tpy-SMe (dashed blue line in Figure 1) disappears and a new less-intense fluorescence band ($\tau = 3.5$ ns) at 500 nm is observed (Table 1, Supporting Information Figure S9).

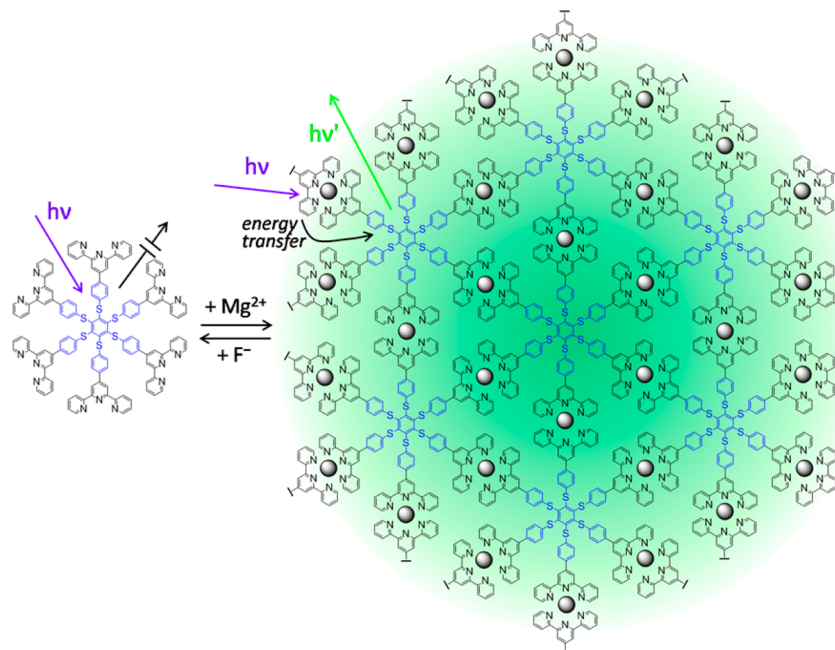
In summary, the unexpected results obtained for compound **1** upon titration with Mg^{2+} ions are (i) a plateau of absorbance and emission intensity values at 3 equiv of metal ion per **1** and (ii) the appearance of the core phosphorescence in fluid solution, whereas for molecule **2**, phosphorescence is observed only in rigid environment. These results can be interpreted on the basis of the formation of a polymeric self-assembled structure in which each metal ion is coordinated by two tpy ligands of two different molecules. Indeed, Mg^{2+} ions are

Table 1. Most Relevant Photophysical Data of **1**, **2** and tpy-SMe in Air-Equilibrated THF Solution (unless Otherwise Noted) at 298 K

	absorption		emission		
	$\lambda_{\text{max}}/\text{nm}$	$\epsilon/10^4 \text{ M}^{-1} \text{ cm}^{-1}$	$\lambda_{\text{max}}/\text{nm}$	Φ_{em}	$\tau/\mu\text{s}$
tpy-SMe	297	3.7	388	0.52	1.4×10^{-3}
$[\text{Mg}(\text{tpy-SMe})_2]^{2+}$	346	5.3	500	0.25	3.5×10^{-3}
1	283	17.8	550 ^a	0.02 ^a	1.7, 11.6 ^a
$[\text{Mg}_5(\text{1})]^{6+}$	289		545	0.10	1.7, 5.3
2	326	19.2	513 ^a	1.00 ^a	3.0 ^a

^aIn the solid state, as a powder.

Scheme 2



known to form complexes with tpy ligands in a 1:2 metal to ligand stoichiometry.²² The formation of a complex in which two tpy units of the same molecule binds a metal ion is prevented for geometric reasons. A very simplistic 2D representation of the self-assembled structure is presented in Scheme 2. Although the structure is represented on a plane, it is not realistic. It is expected that a low-energy conformer would position the tpy arms in a 3D radial extension, in an alternating up and down pattern from the plane of the central benzene core.²³

As evidenced by this picture, intramolecular rotation and motion are strongly hindered upon formation of the self-assembled structure, and this results in a phosphorescent system in fluid solution. The phosphorescence quantum yield and the corresponding lifetime is poorly sensitive to the presence of dioxygen, in agreement with a polymeric structure in which oxygen diffusion is also hindered.

Another interesting feature of this supramolecular polymer is that it performs as an extremely efficient light-harvesting antenna: upon excitation of the $[\text{Mg}(\text{tpy})_2]^{2+}$ units sensitization of the phosphorescence of the hexathiobenzene core takes place with >90% efficiency (see Supporting Information Figure S10). This is demonstrated by the close match between the excitation spectrum recorded at $\lambda_{\text{em}} = 550$ nm and the absorption spectrum both recorded for a solution of **1** with 3.5 equiv of Mg^{2+} ions (Supporting Information Figure S11).

The thusly obtained supramolecular structure can be disassembled upon addition of tetrabutylammonium fluoride (TBAF) to the THF solution because fluoride anions sequester Mg^{2+} cations, forming MgF_2 , characterized by very low solubility ($K_{\text{ps}} = 6.5 \times 10^{-9}$ in water).²⁴ Therefore, molecule **1** performs not only as a turn-on phosphorescent sensor of Mg^{2+} ions, but also as a turn-off phosphorescent sensor of F^- anions (see absorption and emission spectral changes reported in Supporting Information Figure S12). The sensing process is reversible (Scheme 2) because the phosphorescence of the system can be switched on and off upon successive additions of Mg^{2+} and F^- ions.

To further ascertain the formation of a polymeric structure, dynamic light scattering (DLS) experiments were performed under the same experimental conditions of the spectrophotometric titration. The formation of relatively monodispersed aggregates are evidenced upon addition of Mg^{2+} ions. The increasing size of the aggregates reaches a plateau at the end of the titration (3.5 equiv of metal ions per **1**) with an average diameter of ca. 60 nm and a polydispersity index (PDI) of 0.06 (Figure 3a and Supporting Information Figure S13). These aggregates do not dissociate upon addition of an excess of metal ions up to 6 equiv relative to **1**.

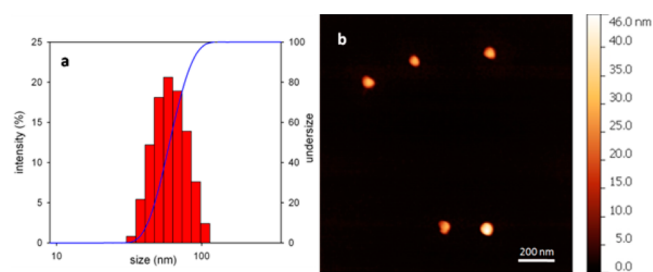


Figure 3. (a) Size distribution by DLS analysis on a 3.3×10^{-6} M THF solution of **1** after addition of 3.5 equiv of $\text{Mg}(\text{ClO}_4)_2$. The red line refers to the cumulative frequency distribution of the size of the nanoparticles. (b) AFM peak force mode image of the same solution spin-coated on freshly cleaved mica.

A 3.3×10^{-6} M solution of **1** in THF with 3.5 equiv of Mg^{2+} was spin-coated on freshly cleaved mica. Figure 3b reports an AFM image of a selected area. The particle distribution based on a larger image containing ca. 30 nanoparticles shows a height of ca. 40 nm and a mean diameter of 50 nm, in good agreement with the data obtained by DLS analysis.

Because of the interesting results obtained upon complexation of Mg^{2+} ions, a screening of different metal ions was performed: a 6.1×10^{-6} M solution of **1** was titrated with mM solutions of $\text{Ca}(\text{ClO}_4)_2$, $\text{Mg}(\text{ClO}_4)_2$, $\text{Fe}(\text{CF}_3\text{SO}_3)_2$, $\text{Co}(\text{ClO}_4)_2$,

Ni(CF₃SO₃)₂, Cu(CF₃SO₃)₂, Zn(CF₃SO₃)₂, Cd(ClO₄)₂. The absorption spectra at the end of the titration (3.5 equiv of metal ions per **1**) show red-shifted absorption maxima compared to the free ligand for all the investigated metal ions and a new metal-to-ligand charge-transfer (MLCT) band²⁵ in the visible region upon addition of Fe²⁺ (Supporting Information Figure S13). Supporting Information Figure S14 reports the emission intensities upon excitation at 327 nm for a solution of **1** in the presence of 3.5 equiv of the different metal ions. As expected, no phosphorescence is recorded upon addition of Fe²⁺, Co²⁺, Ni²⁺, and Cu²⁺ because of photoinduced energy/electron transfer processes between the phosphorescent core and the metal complexes at the periphery. Indeed, these metal ions display low energy excited states and can be involved in electron transfer processes. In the case of Ca²⁺, Zn²⁺, and Cd²⁺, which are d⁰ or d¹⁰ metal ions, energy and electron transfer processes are not favored, so that the same phosphorescence band observed for Mg²⁺ complexes is present with a lower emission quantum yield.

CONCLUSIONS

The phosphorescence of **1** can be switched on upon complexation of appropriate divalent metal ions. Particularly interesting results are obtained for Mg²⁺; a supramolecular polymer is formed, and it exhibits the highest emission quantum yield (10%) among the investigated metal ions, with microsecond-excited state lifetime in air-equilibrated THF solution. It performs as a very efficient light-harvesting antenna. The supramolecular polymer can be disassembled upon addition of fluoride anions which sequester Mg²⁺ ions, yielding a reversible switch off of the phosphorescence. This example represents a new paradigm in luminescent sensors since the emission signal is not directly related to the metal complex property. To the contrary, it results from a self-assembled supramolecular architecture, which slows down intramolecular motions of the core chromophore of the multivalent ligand **1**. Those factors leading to a molecular rigidity provide a new phosphorescence-based system with AIE activities and phosphorescent supramolecular sensors for both cations and anions, which is exceptional.

ASSOCIATED CONTENT

Supporting Information

Detailed experimental procedures and additional figures. This material is available free of charge via the Internet at <http://pubs.acs.org>.

AUTHOR INFORMATION

Corresponding Authors

paola.ceroni@unibo.it
marc.gingras@univ-amu.fr

Notes

The authors declare no competing financial interest.

ACKNOWLEDGMENTS

This work was financially supported by the European Research Council ERC-StG (PhotoSi, 278912), MIUR (FIRB RBAP11C58Y, PRIN 2010N3T9M4) in Italy, the French National Center for Scientific Research (CNRS), Aix-Marseille Université, and the French-Italian University for a Ph.D. scholarship to A.F. from the Vinci program.

REFERENCES

- (1) Schubert, U. S.; Hofmeier, H.; Newkome, G. R. *Modern Terpyridine Chemistry*; Wiley-VCH: Weinheim, Germany, 2006.
- (2) (a) Wild, A.; Winter, A.; Schlütter, F.; Schubert, U. S. *Chem. Soc. Rev.* **2011**, *40*, 1459. (b) Constable, E. C. *Chem. Soc. Rev.* **2007**, *36*, 246.
- (3) Flamigni, L.; Collin, J.-P.; Sauvage, J.-P. *Acc. Chem. Res.* **2008**, *41*, 857.
- (4) (a) Machan, C. W.; Adelhart, M.; Sarjeant, A. A.; Stern, C. L.; Sutter, J.; Meyer, K.; Mirkin, C. A. *J. Am. Chem. Soc.* **2012**, *134*, 16921. (b) Barigelletti, F.; Flamigni, L. *Chem. Soc. Rev.* **2000**, *29*, 1.
- (5) (a) Glasson, C. R. K.; Lindoy, L. F.; Meehan, G. V. *Coord. Chem. Rev.* **2008**, *252*, 940. (b) Puntoriero, F.; Campagna, S.; Stadler, A. M.; Lehn, J.-M. *Coord. Chem. Rev.* **2008**, *252*, 2480.
- (6) For some recent examples, see (a) Lu, X.; Li, X.; Cao, Y.; Schultz, A.; Wang, J.-L.; Moorefield, C. N.; Wesdemiotis, C.; Cheng, S. Z. D.; Newkome, G. R. *Angew. Chem., Int. Ed.* **2013**, *52*, 7728. (b) Schultz, A.; Li, X.; Barkakaty, B.; Moorfield, C. N.; Wesdemiotis, C.; Newkome, G. R. *J. Am. Chem. Soc.* **2012**, *134*, 7672. (c) Chan, Y.-T.; Li, X.; Yu, J.; Carri, G. A.; Moorefield, C. N.; Newkome, G. R.; Wesdemiotis, C. *J. Am. Chem. Soc.* **2011**, *133*, 11967. (d) Wang, J.-L.; Li, X.; Lu, X.; Hsieh, I.-F.; Cao, Y.; Moorefield, C. N.; Wesdemiotis, C.; Cheng, S. Z. D.; Newkome, G. R. *J. Am. Chem. Soc.* **2011**, *133*, 11450.
- (7) (a) Andres, P. R.; Schubert, U. S. *Adv. Mater.* **2004**, *16*, 1043. (b) Schubert, U. S.; Eschbaumer, C. *Angew. Chem., Int. Ed.* **2002**, *41*, 2892.
- (8) For some recent examples, see (a) Wang, C.; Hao, X.-Q.; Wang, M.; Guo, C.; Xu, B.; Tan, E. N.; Zhang, Y.-Y.; Yu, Y.; Li, Z.-Y.; Yang, H.-B.; Song, M.-P.; Li, X. *Chem. Sci.* **2014**, *5*, 1221. (b) Zhan, J.; Hu, Q.; Wu, Q.; Li, C.; Qiu, H.; Zhang, M.; Yin, S. *Chem. Commun.* **2014**, *50*, 722. (c) Molloy, J. K.; Ceroni, P.; Venturi, M.; Bauer, T.; Sakamoto, J.; Bergamini, G. *Soft Matter* **2013**, *9*, 10754. (d) Zhang, K.; Zha, Y.; Peng, B.; Chen, Y.; Tew, G. N. *J. Am. Chem. Soc.* **2013**, *135*, 15994. (e) Bauer, T.; Zheng, Z.; Renn, A.; Enning, R.; Stemmer, A.; Sakamoto, J.; Schlüter, A. D. *Angew. Chem., Int. Ed.* **2011**, *50*, 7879. (f) Eryazici, I.; Farha, O. K.; Compton, O. C.; Stern, C.; Hupp, J. T.; Nguyen, S. T. *Dalton Trans.* **2011**, *40*, 9189.
- (9) Albano, G.; Balzani, V.; Constable, E. C.; Maestri, M.; Smith, D. R. *Inorg. Chim. Acta* **1998**, *277*, 225.
- (10) (a) Hong, Y.; Lam, J. W. Y.; Tang, B. Z. *Chem. Soc. Rev.* **2011**, *40*, 5361. (b) Hong, Y.; Lam, J. W. Y.; Tang, B. Z. *Chem. Commun.* **2009**, 4332 and references therein.
- (11) (a) Virgili, T.; Forni, A.; Cariati, E.; Pasini, D.; Botta, C. *J. Phys. Chem. C* **2013**, *117*, 27161. (b) Yuan, W. Z.; Shen, X. Y.; Zhao, H.; Lam, J. W. Y.; Tang, L.; Lu, P.; Wang, C.; Liu, Y.; Wang, Z.; Zheng, Q.; Sun, J. Z.; Ma, Y.; Tang, B. Z. *J. Phys. Chem. C* **2010**, *114*, 6090.
- (12) (a) Shustova, N. B.; Cozzolino, A. F.; Dincă, M. *J. Am. Chem. Soc.* **2012**, *134*, 19596. (b) Yin, S.; Zhang, J.; Feng, H.; Zhao, Z.; Xu, L.; Qiu, H.; Tang, B. *Dyes Pigm.* **2012**, *95*, 174. (c) Shustova, N. B.; McCarthy, B. D.; Dincă, M. *J. Am. Chem. Soc.* **2011**, *133*, 20126. (d) Xu, B.; Chi, Z.; Zhang, X.; Li, H.; Chen, C.; Liu, S.; Zhang, Y.; Hu, J. *Chem. Commun.* **2011**, *47*, 11080.
- (13) Bergamini, G.; Fermi, A.; Botta, C.; Giovanella, U.; Di Motta, S.; Negri, F.; Peresutti, R.; Gingras, M.; Ceroni, P. *J. Mater. Chem. C* **2013**, *1*, 2717.
- (14) The previously published emission quantum yield of 0.8 was underestimated because the sample was not completely crystalline.
- (15) Demas, J. N.; Crosby, G. A. *J. Phys. Chem.* **1971**, *75*, 991.
- (16) In *Handbook of Photochemistry*, 3rd ed.; Montalti, M.; Credi, A.; Prodi, L.; Gandolfi, M. T. Eds.; Taylor & Francis: London, 2006; Ch. 10.
- (17) De Mello, J. C.; Wittmann, H. F.; Friend, R. H. *Adv. Mater.* **1997**, *9*, 230.
- (18) Review on aromatic persulfuration: Gingras, M.; Raimundo, J.-M.; Chabre, Y. M. *Angew. Chem., Int. Ed.* **2006**, *45*, 1686.
- (19) The protocol was improved with *t*-BuOK instead of powdered NaH. (a) Van Bierbeek, A.; Gingras, M. *Tetrahedron Lett.* **1998**, *39*,

6283. (b) Pinchart, A.; Dallaire, C.; Gingras, M. *Tetrahedron Lett.* **1998**, *39*, 543.

(20) See, for example, (a) Tuccitto, N.; Torrisi, V.; Cavazzini, M.; Morotti, T.; Puntoriero, F.; Quici, S.; Campagna, S.; Licciardello, A. *ChemPhysChem* **2007**, *8*, 227. (b) Constable, E. C.; Lewis, J.; Liptrot, M. C.; Raithby, P. R. *Inorg. Chim. Acta* **1990**, *178*, 47.

(21) Tucker, J. H. R.; Gingras, M.; Brand, H.; Lehn, J.-M. *J. Chem. Soc., Perkin Trans. 2* **1997**, 1303.

(22) Constable, E. C.; Healy, J.; Drew, M. G. B. *Polyhedron* **1991**, *10*, 1883–1887.

(23) X-ray crystallographic data of hexakis(phenylthio)benzene indicated alternating phenyl rings above and below the plane of the central benzene core: (a) MacNicol, D. D.; Wilson, D. R. *J. Chem. Soc. Chem. Commun.* **1976**, 494. (b) MacNicol, D. D.; Hardy, A. D. U.; Wilson, D. R. *Nature* **1977**, *266*, 611. Moreover, calculations by the GenMol program established that a thiophenylated benzene core displays a 3D architecture: Aubert, C.; Dallaire, C.; Pèpe, G.; Levillain, E.; Félix, G.; Gingras, M. *Eur. J. Org. Chem.* **2012**, 6145.

(24) Clifford, A. F. *Inorganic Chemistry of Qualitative Analysis*; Prentice-Hall, Inc.: Upper Saddle River, NJ, 1961.

(25) Braterman, P. S.; Song, J.-I.; Peacock, R. D. *Inorg. Chem.* **1992**, *31*, 555 and references therein.

■ NOTE ADDED AFTER ASAP PUBLICATION

The first paragraph of the Results and Discussion section has been corrected. The revised version was re-posted on April 30, 2014.